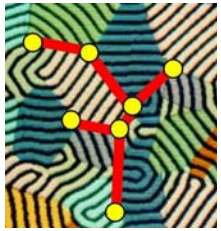

METRO
MEtallurgical TRaining On-line

IPPT PAN

Solidification / microsegregation model applied to description of diffusion soldering / brazing

Waldemar Wołczyński
IMMS PAS

Education and Culture

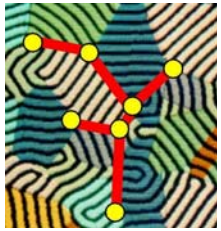

Non-equilibrium solidification Scheil's theory

Scheil's theory for the non-equilibrium solidification / microsegregation

solute concentration in the liquid → $N_L(x;0) = N_0(1-x)^{k-1}$

solute concentration at s/l interface → $N_S(x,0) = kN_0(1-x)^{k-1}$

solute redistribution in the solid → $N_B(x,0) = kN_0(1-x)^{k-1}$

redistribution is a result of back-diffusion, but no diffusion in the solid according to the Scheil's model, thus $\alpha = 0$, and $N_B(x,0) = N_S(x,0)$

E. Scheil, Zeitschrift fur Metallkunde, 34, (1942), 70-80

Non-equilibrium solidification
Multi-peritectic systems

Scheil's model for the non-equilibrium solidification / microsegregation can be developed for multi-peritectic or multi-peritectic/eutectic systems

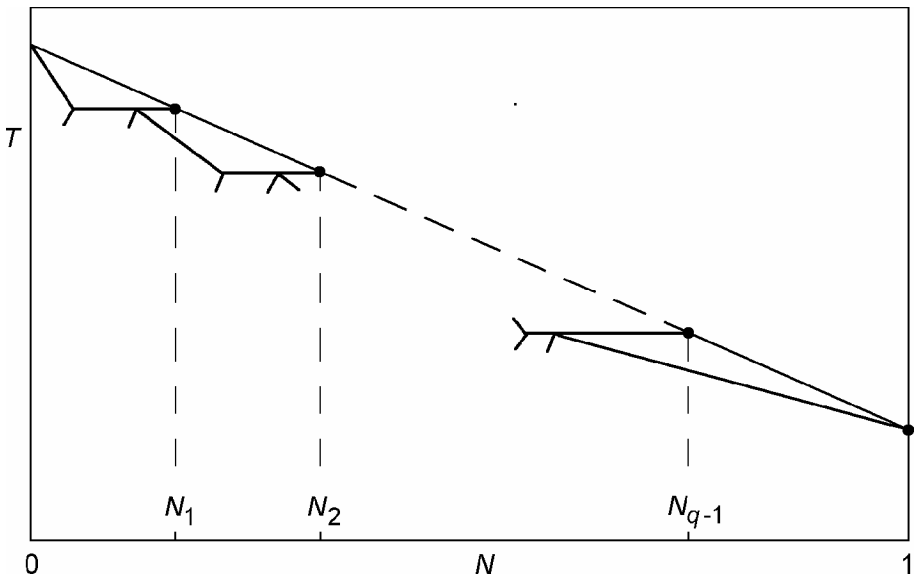

FIG. 1

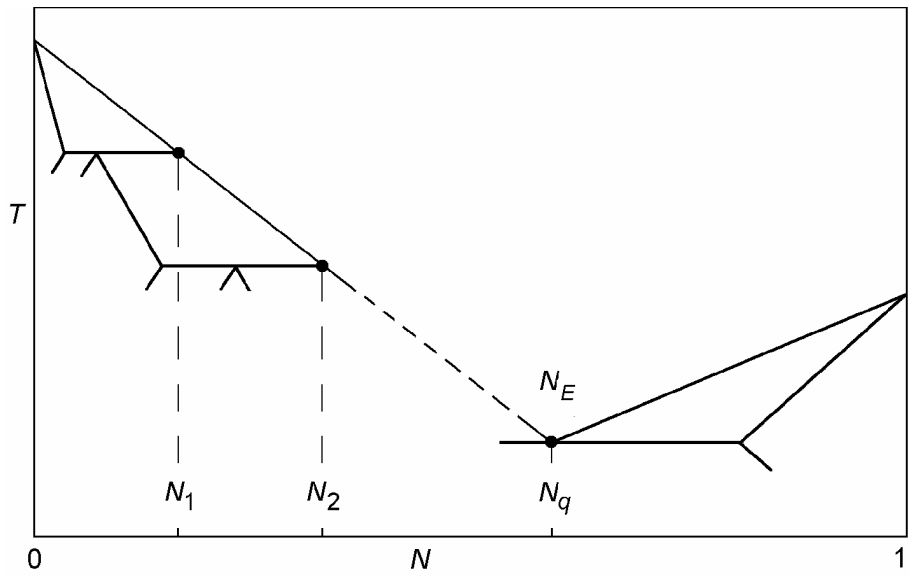

FIG. 2

arbitrary phase diagram: multi-peritectic system, FIG. 1
multi-peritectic eutectic system, FIG. 2

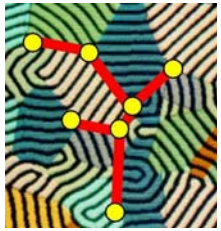

Non-equilibrium solidification Solute behaviour

Scheil's model for the non-equilibrium solidification / microsegregation is now developed for multi-peritectic or multi-peritectic eutectic systems

solute concentration in the liquid →

$$N_L(x;0) = N_{i-1}\left(\frac{1-x}{1-x_{i-1}}\right)^{k_{i-1}}$$

solute concentration at s/l interface →

$$N_S(x;0) = k_i N_{i-1}\left(\frac{1-x}{1-x_{i-1}}\right)^{k_{i-1}}$$

solute redistribution in the solid →

$$N_B(x;0) = k_i N_{i-1}\left(\frac{1-x}{1-x_{i-1}}\right)^{k_{i-1}}$$

x amount of the growing solid, dimensionless $x \in [x_{i-1}, x_i]$ $i = 1,\ldots, q$

Non-equilibrium solidification Initial conditions

Scheil's model for the non-equilibrium solidification / microsegregation is now developed for multi-peritectic or multi-peritectic eutectic systems

$$\frac{dN_L(x,0)}{dx} = N_L(x,0)\frac{1-k}{1-x}$$

travelling initial condition
$N_0(x_0)$, $N_1(x_1)$ …
is applied to above differential equation

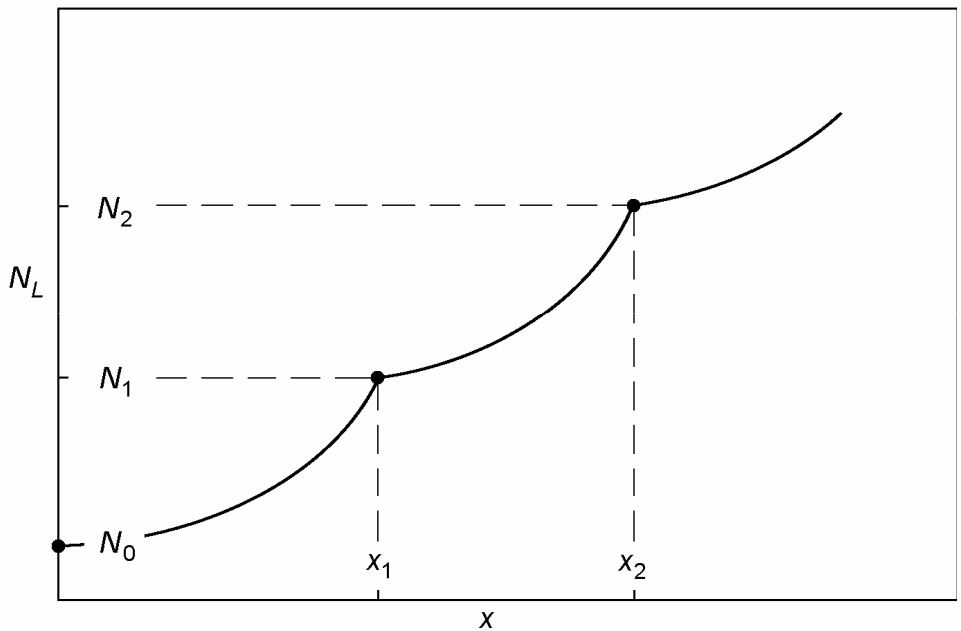

FIG. 3

W.Wołczyński, Chapter 2 in: Modelling of Transport Phenomena in Crystal Growth, eds. J.Szmyd & K.Suzuki, ed. WIT Press, Southampton, Boston, (2000), p. 19-59

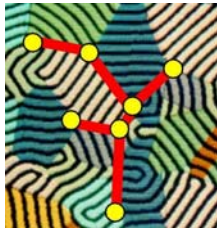

Non-equilibrium solidification Amount of the solid

Scheil's model for the non-equilibrium solidification / microsegregation is now developed for multi-peritectic or multi-peritectic eutectic systems

$$x_i = 1 - \left(N_0\right)^{\frac{1}{1-k_1}} \left(N_i\right)^{\frac{1}{k_i - 1}} \prod_{j=1}^{i-1} \left(N_j\right)^{\frac{1}{k_j - 1} - \frac{1}{k_{j+1} - 1}} \qquad i = 2,\ldots, q$$

$$k = \frac{N_S\left(x;0\right)}{N_L\left(x;0\right)}$$ partition ratio for q = 1

k_i $\quad i = 1,\ldots, q$ partition ratio, generally

x_i $\quad i = 1,\ldots, q$ amount of the primary solid at a given peritectic reaction

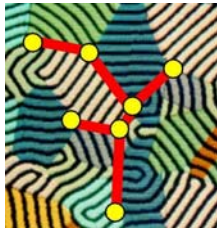

Equilibrium solidification

solute concentration in the liquid → $N_L(x;1) = N_0(1+kx-x)^{-1}$

solute concentration at s/l interface → $N_S(x;1) = kN_0(1+kx-x)^{-1}$

solute redistribution in the solid → $N_B(1;1) = N_0$

a general description of solidification/microsegregation is required !

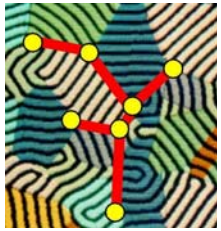

General theory for solidification / microsegregation Brody-Flemings theory

a general theory has already been proposed by Brody and Flemings, but according to the theory, back-diffusion parameter tends to infinity: $\alpha \rightarrow \infty$ moreover, no description for the solute redistribution in the solid is given and mass balance is not satisfied

however, back-diffusion parameter should tend to unity: $\alpha \rightarrow 1$

$$\alpha = \frac{D_S\, t_f}{L^2} \quad \rightarrow \quad \alpha = \frac{t_f}{t_d} \qquad \text{with} \qquad t_d = \frac{L^2}{D_S}$$

really, when $t_f = t_d$ then $\alpha = 1$,

t_f local solidification time, t_d time necessary for homogenization

RESULT *a general description of solidification/microsegregation is always required !*

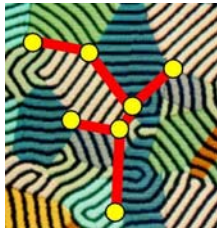

General theory for solidification / microsegregation

solute concentration in the liquid ➔ $N_L(x;\alpha) = N_0(1+\alpha k x - x)^{\frac{k-1}{1-\alpha k}}$

solute concentration at s/l interface ➔ $N_S(x;\alpha) = kN_0(1+\alpha k x - x)^{\frac{k-1}{1-\alpha k}}$

solute redistribution in the solid $N_B(x;x_0,\alpha) = N_S(x;\alpha) + \beta_{ex}(x;x_0)\beta_{in}(x_0,\alpha)N_L(x;\alpha)$

$x \in [0, x_K]$ $x_0 \in [0, x_K]$ $\beta(x;x_0,\alpha) = \beta_{ex}(x;x_0)\beta_{in}(x_0,\alpha)$ $0 \le \alpha \le 1$

x_0 parameter representing freezing ≡ amount of the solid when solidification is arrested

W.Wołczyński, Chapter 2 in: Modelling of Transport Phenomena in Crystal Growth, eds. J.Szmyd & K.Suzuki, ed. WIT Press, Southampton, Boston, (2000), p. 19-59

Generalization

proposed equations are reducible to: Scheil's equations for $\alpha = 0$ and description of equilibrium solidification for $\alpha = 1$

$$N_S^{\beta}(x; x_K, \alpha) \equiv N_B(x; x_K, \alpha)$$

$$(\alpha_E k)^{\frac{k-1}{1-\alpha_E k}} = \frac{N_E}{N_0}$$

FIG. 4

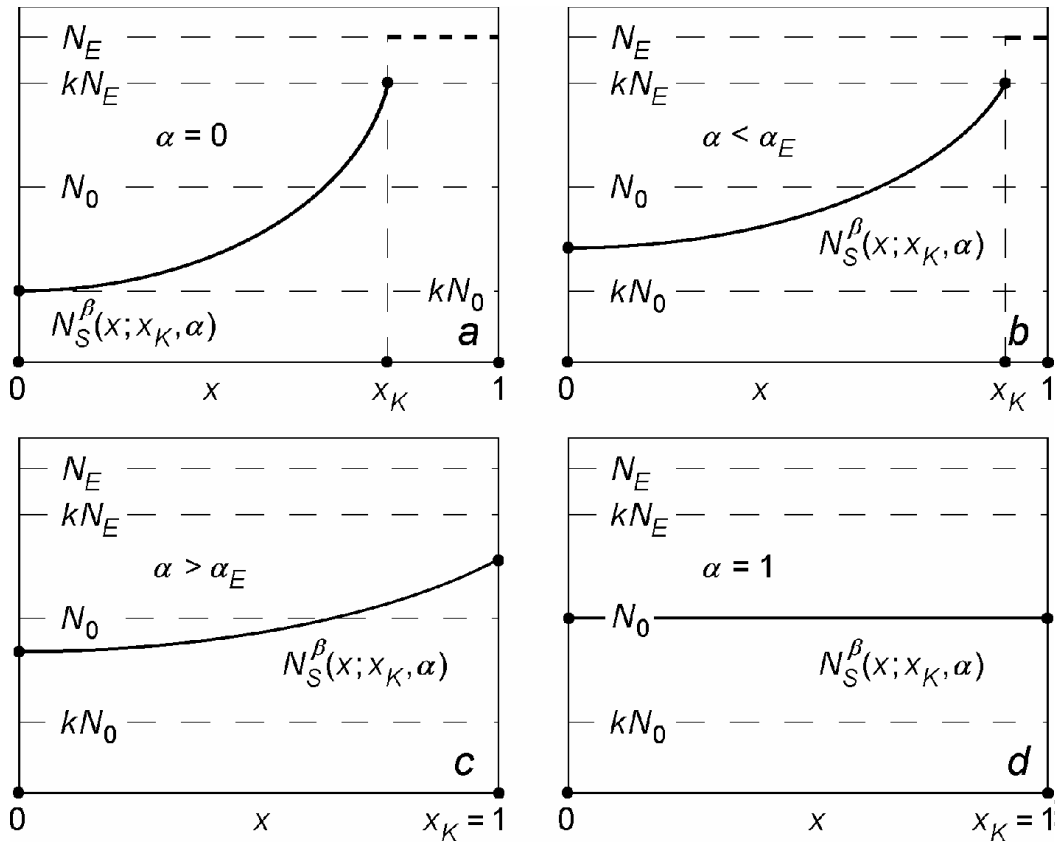

schematic view of solute redistribution for four representative values of back-diffusion parameter

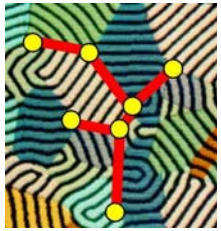

Diffusion soldering / brazing Phenomena

 # dissolution
 # solidification
 # solid / solid transformations

#
dissolution prepares initial solution within zone, *dx*
for solidification
#
solidification forms sub-layers within the solder/braze
#
solid/solid transformations usually occur after
completion of both phenomena: dissolution + solidification

- solute concentration of the initial solution is equal to: N_0
- zone *dx* is formed by dissolution just at the surface of a substrate, perpetually
- next, solidification of a given zone *dx*, is expected
- some reactions occur during solidification !!!

Solid / liquid interface

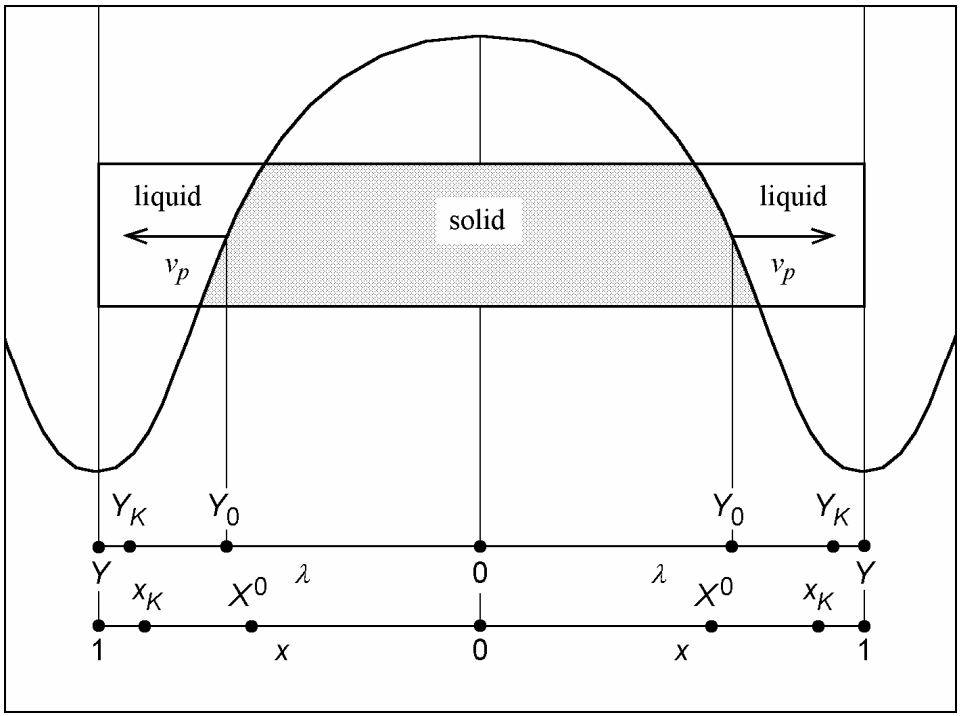

2D *solidification formation of cellular morphology*

FIG. 5

x current amount of the growing solid (layer) $0 < x < x_K$

X^0 amount of solid (layer) for which solidification is stopped and morphology frozen

x_K amount of solid (layer) just before precipitation of the so-called last droplet of the liquid (eutectic)

Distance

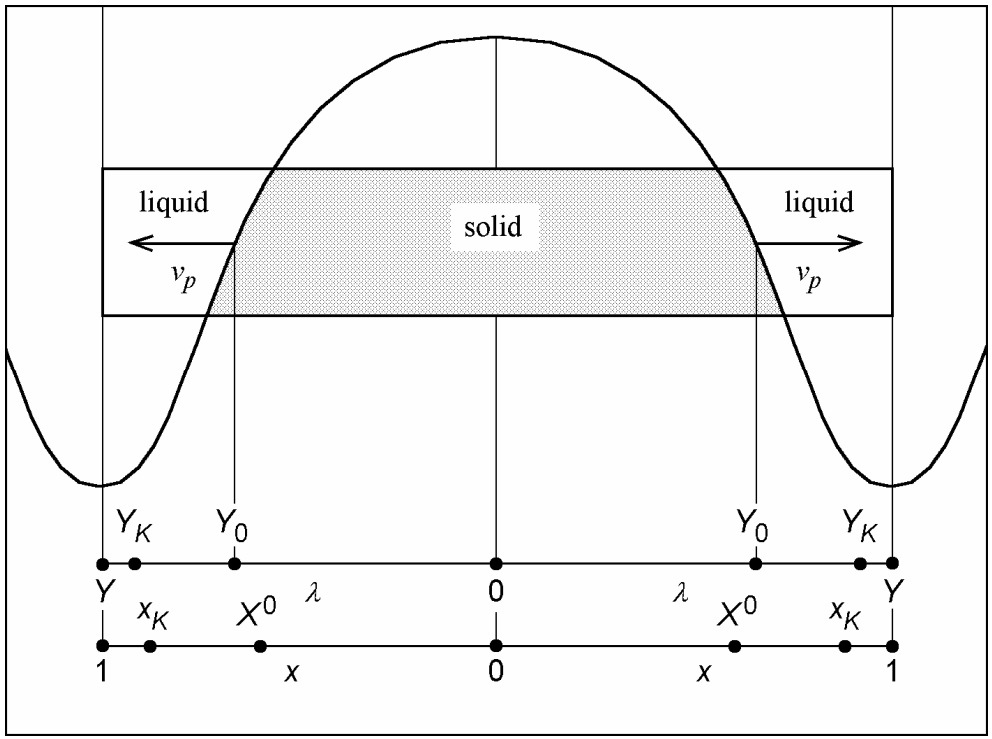

2D solidification formation of cellular morphology

FIG. 6

λ distance from the axis of symmetry of a given cell

Y^0 distance at which solidification is arrested and morphology frozen

Y_K solid / precipitate boundary

Application of 2D model to 1D model of multi-layer formation

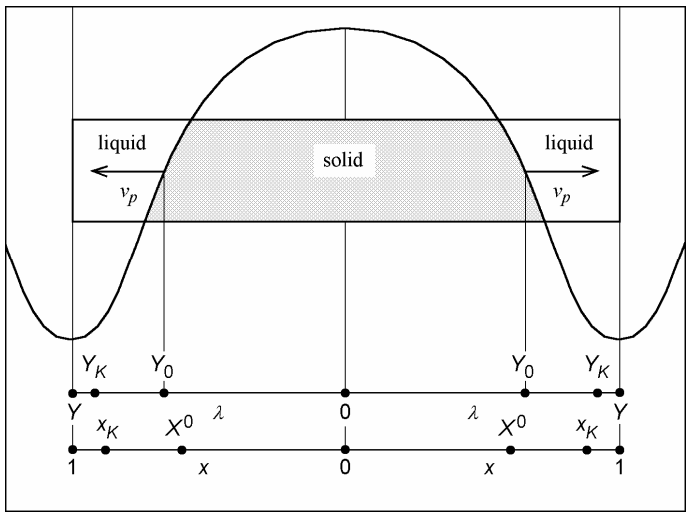

FIG. 7

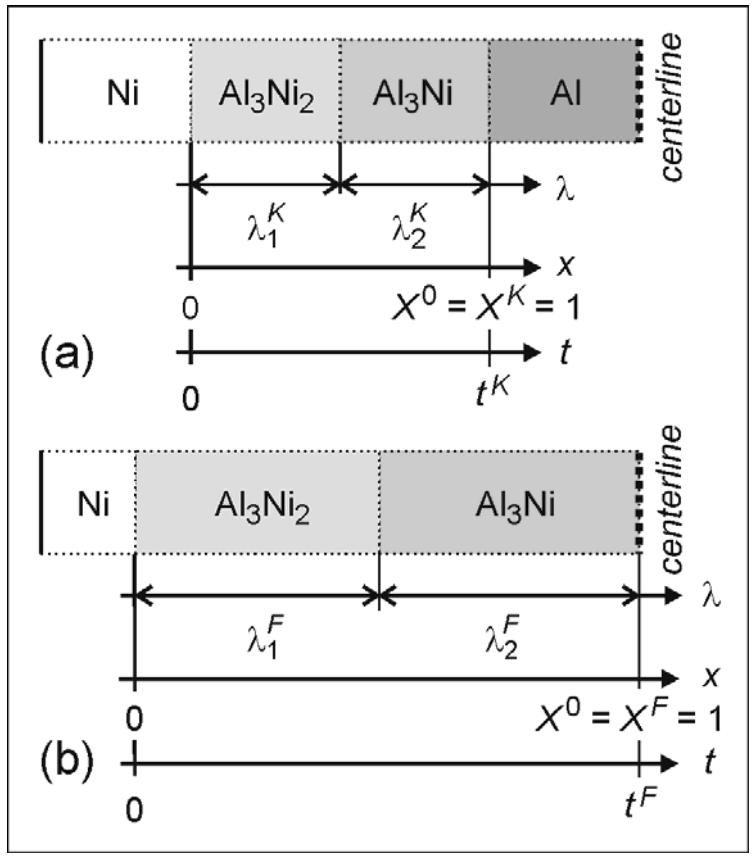

FIG. 8

2D *solidification formation of cellular morphology*

λ distance from the substrate surface

$X^0 = 1$ amount of multi-layer at which solidification is stopped and morphology frozen

t^F time of the completion of solidification

1D solidification leading to formation multi-layer

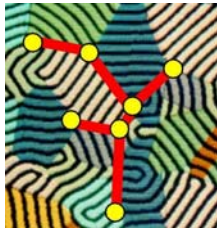

X^0, L^0 Model 2D

amount of the arrested solid within i - range of solidification, during diffusion soldering/brazing

$$x_i^0 = \begin{cases} X^0, & i = 1; \\ X^0 - \sum_{j=1}^{i-1} x_j^{max}, & i = 2,...,n; \end{cases}$$

$$l_i^0 = \begin{cases} L^0, & i = 1; \\ L^0 - \sum_{j=1}^{i-1} x_j^{max}, & i = 2,...,n; \end{cases}$$

amount of the liquid at a beginning of i - range of solidification, during diffusion soldering/brazing

a peritectic reaction occurs at the end of a given range, according to a model referred to phase diagram for stable equilibrium

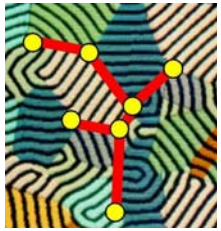

Fundamentals of the „zone *dx*" - model

dissolution leads to ensure N_0 solute concentration within each *dx*

dissolution path:

$N_F \rightarrow N_0$

solidification occurs within each *dx*

solidification path:

$N_0 \rightarrow N_F$

CONCLUSIONS:

no freezing is possible for fraction *dx* !

- therefore $X^0 = 1$, for each *dx*
- when solidification is arrested, $X^0 = 1$, for the sum of all *dx* solidified before arresting

- **the diffusion soldering occurs at a constant temperature, T_R**
- **the liquid solution N^F is not undercooled**
- **the liquid solution N_0 is strongly undercooled**

CONCLUSION !

- **peritectic reactions are undercooled peritectic reactions !**

Real temperature of joining, T_R
Equilibrium temperature, T_L

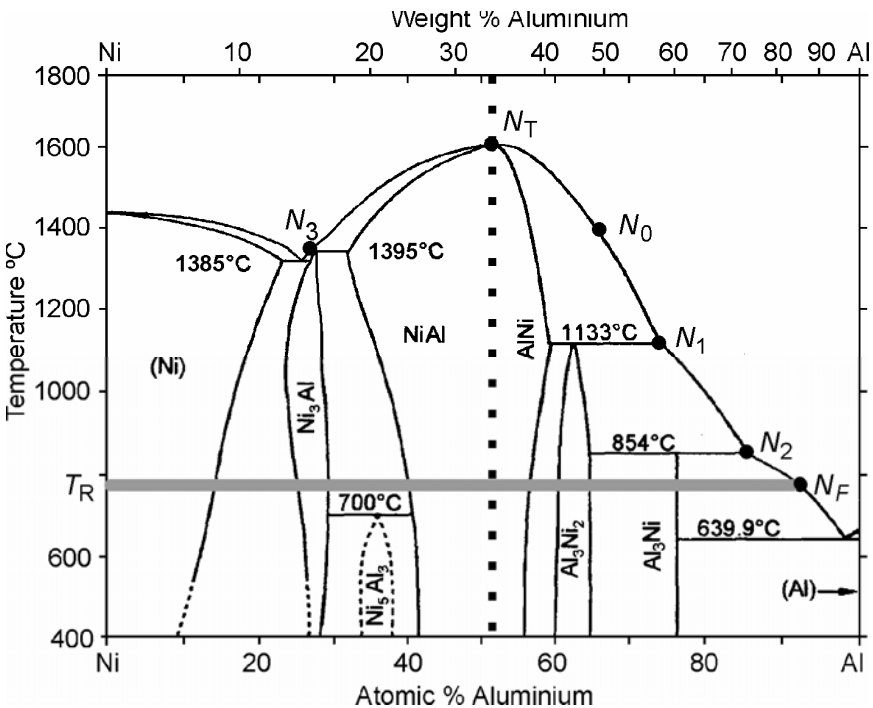

FIG. 9

parameters playing role
in the model
referred
to phase diagram
for stable equilibrium

N_0 – initial content of the solute in the undercooled liquid

N_1 – content of the solute at first peritectic reaction

N_2 – content of the solute at second peritectic reaction

N_F – final content of the solute in the liquid

Driving force for solidification Model Stable equilibrium

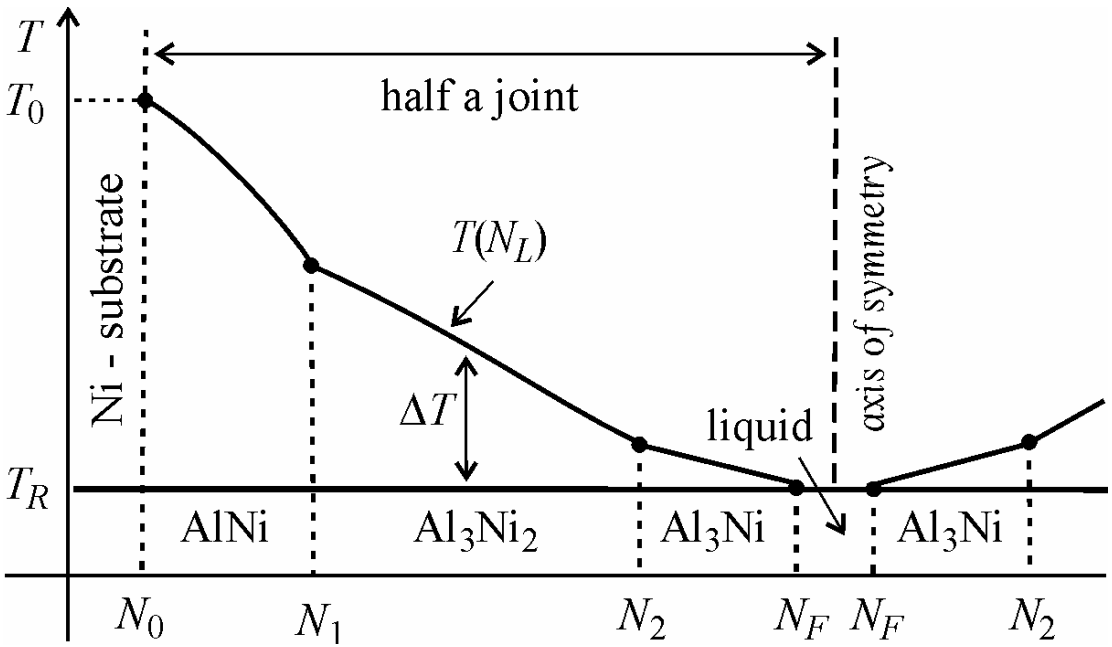

FIG. 10

driving force according to the model based on stable equilibrium

scheme valid for each zone *dx* created during solidification

$$\Delta T = T_L - T_R = T(N_L) - T_R$$

at the N_F - solute content in the liquid solidification process is completed and: $\Delta T = 0$

Initial transient stable formation of the phases

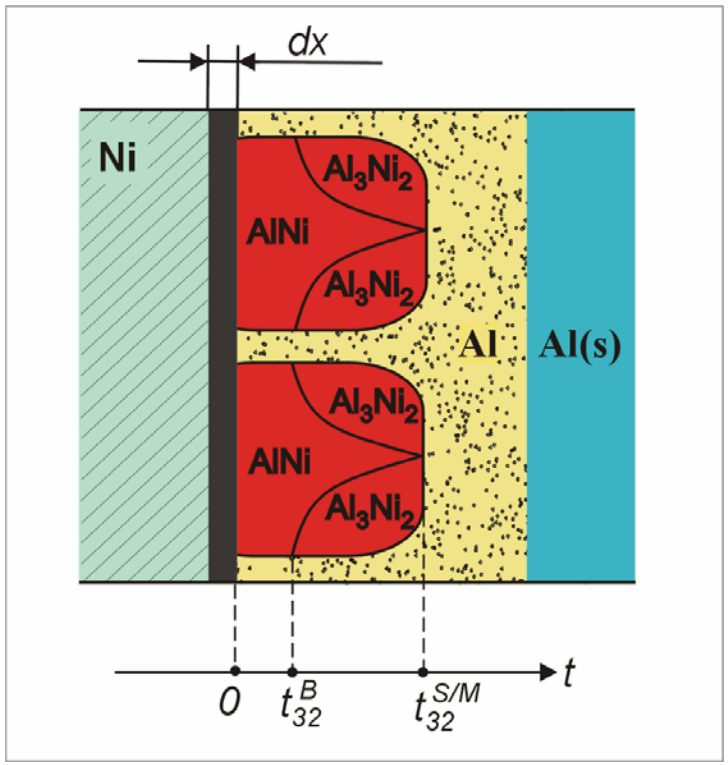

FIG. 11

initial transient period of process

dx is just formed and initial transient solidification begins

- Al-liquid filler metal starts to be melted: Al (s) ➔ Al

- solidification (or birth) of first primary phase AlNi is to be expected at $t_{11}^{B} = 0$

- at time t_{32}^{B} the Al_3Ni_2 birth takes place and stable AlNi phase transforms continuously into the Al_3Ni_2 dominant phase

at time $t_{32}^{S/M}$ stable solidification transforms into metastable process

Competition

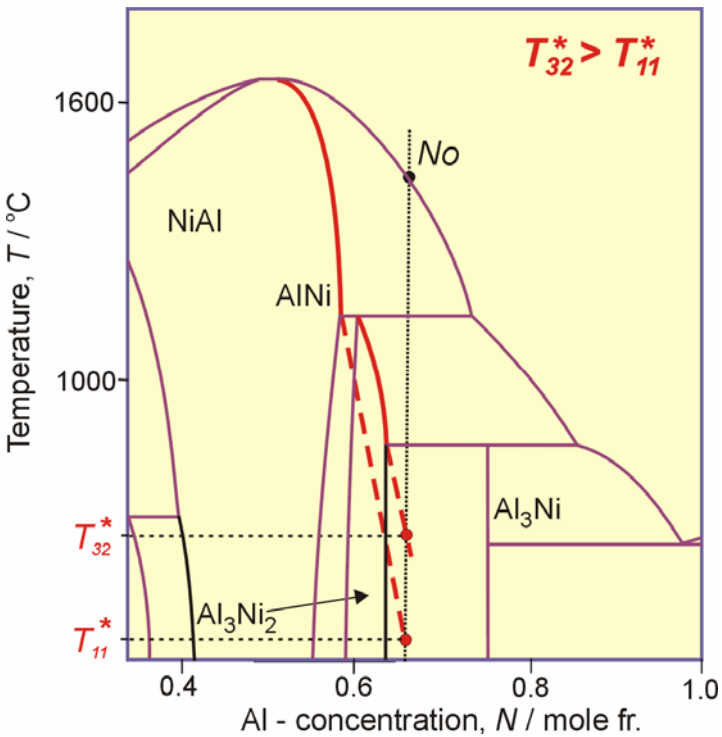

Al_3Ni_2 phase grows instead of AlNi phase

FIG. 12

number of degrees of freedom
f = 0
according to Gibbs Phase Rule

$$f = c - p + 1 = 0$$

since
c = 2 Ni, Al
p = 3 undercooled liquid
within zone *dx*, AlNi, Al_3Ni_2

at time $t_{32}^{S/M}$ competition between initial transient stable solidification and metastable solidification is completed and metastable process begins according to the criterion of maximum temperature of the s / l interface:

$$T^*_{32} > T^*_{11} \quad \text{at} \quad N_0 = \text{const.}$$

Filler metal transformation

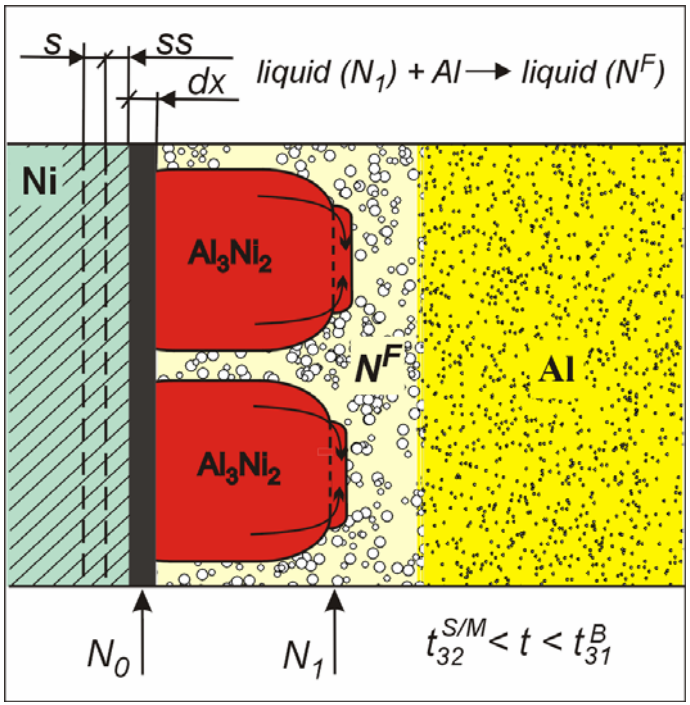

FIG. 13

scheme of the transformation

FIG. 14

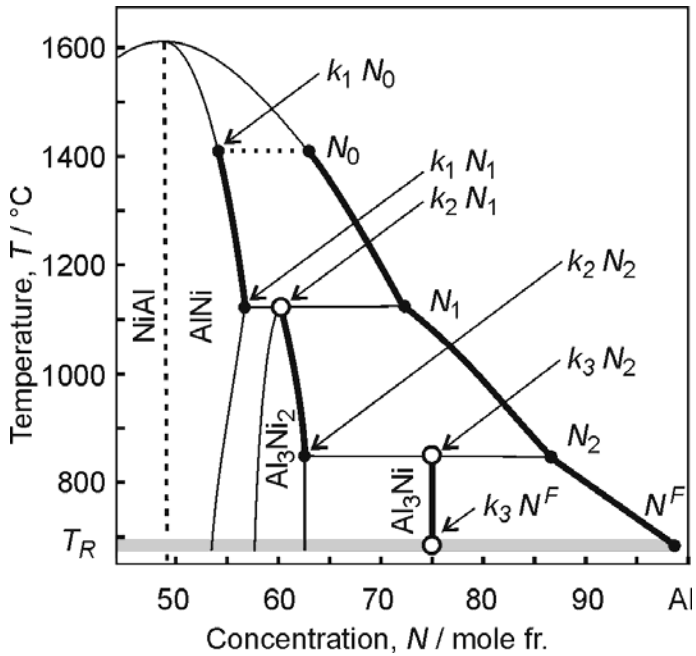

definition of N^F

liquid (N_1) remains after solidification of the dominant Al_3Ni_2 phase

$f = c - p + 1 = 0$
since
$c = 2$ Ni, Al
$p = 3$ dx, Al_3Ni_2, N^F

TRANSFORMATION:

liquid (N_1) + Al → liquid (N^F)

Birth of coupled phase

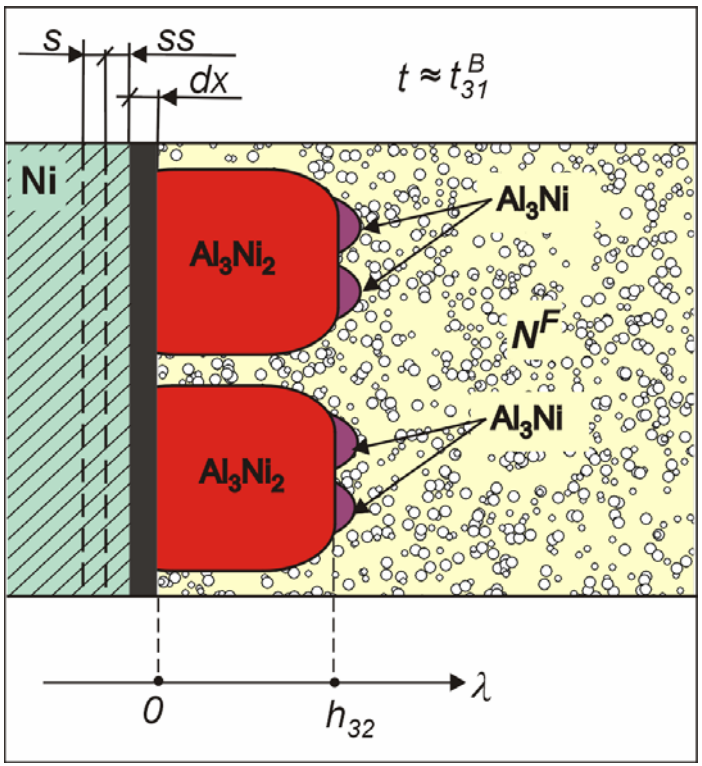

FIG. 15

scheme of the coupled phase birth

number of degrees of freedom
f = 0
according to Gibbs Phase Rule

$f = c - p + 1 = 0$

since

c = 2 Ni, Al
p = 3 undercooled liquid within the zone *dx*, (N_0), Al_3Ni_2 and Al_3Ni

first peritectic phase that is, dominant phase has already its height equal to h_{32}

at time t_{31}^{B} the birth of Al_3Ni phase is observed

Birth of coupled phase Experimental confirmation

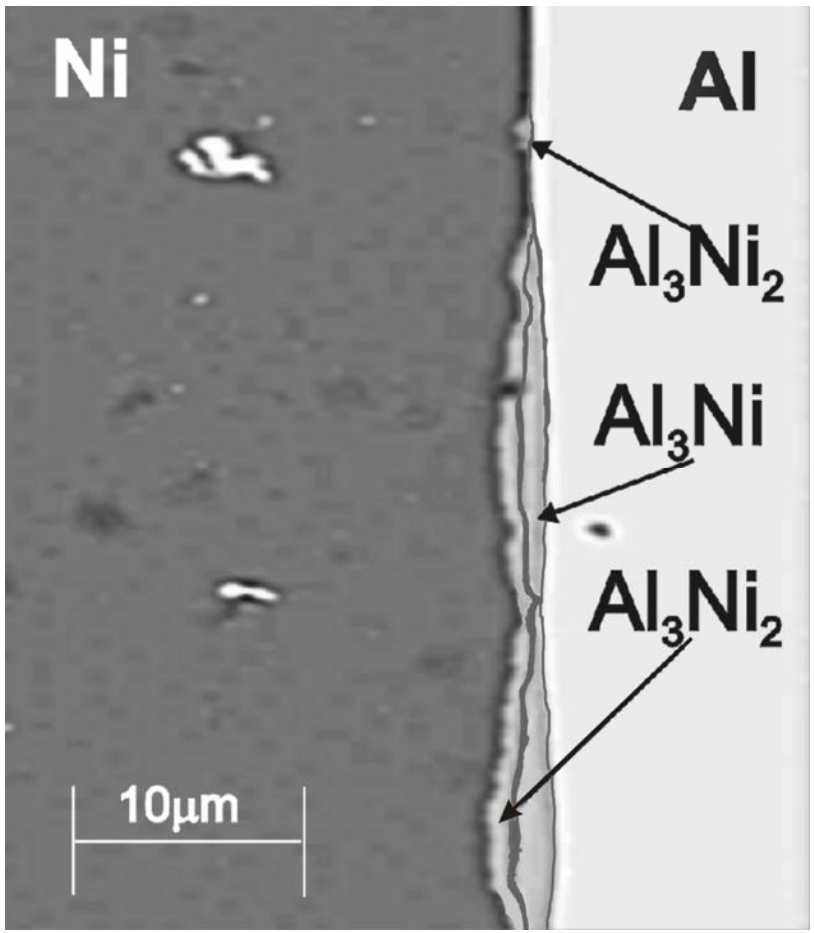

FIG. 16

birth of the coupled phase Al_3Ni on the surface of dominant phase Al_3Ni_2 as observed experimentally

solidification is faster or slower; it depends on the local orientation

← by courtesy of Dr J. Janczak-Rusch, EMPA, Dübendorf, Switzerland

Birth of coupled phase
Experimental confirmation

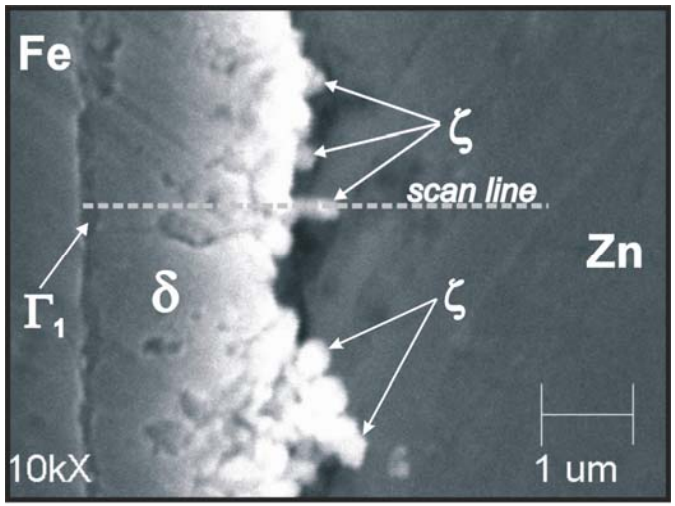

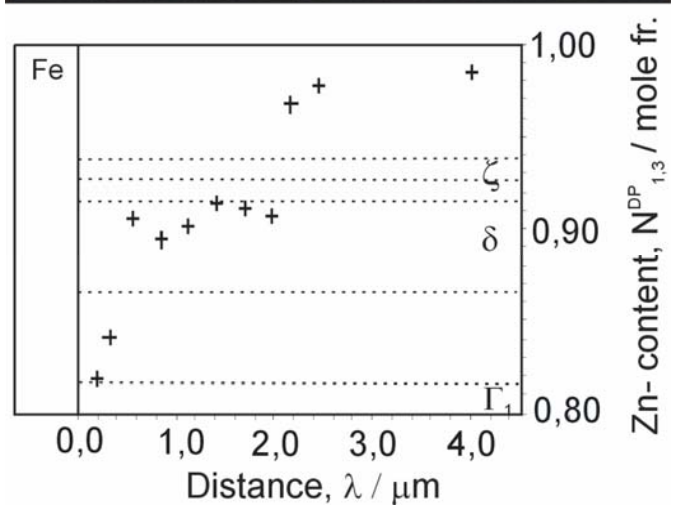

FIG. 17

birth of the coupled phase ζ
on the surface
of dominant phase δ
as observed experimentally

solidification is faster or slower;
it depends on the local orientation

by courtesy of Prof. E.Guzik and Dr D. Kopyciński,
University of Science and Technology,
Kraków, Poland

Perpetual formation of zone, *dx* by the liquid, N^F

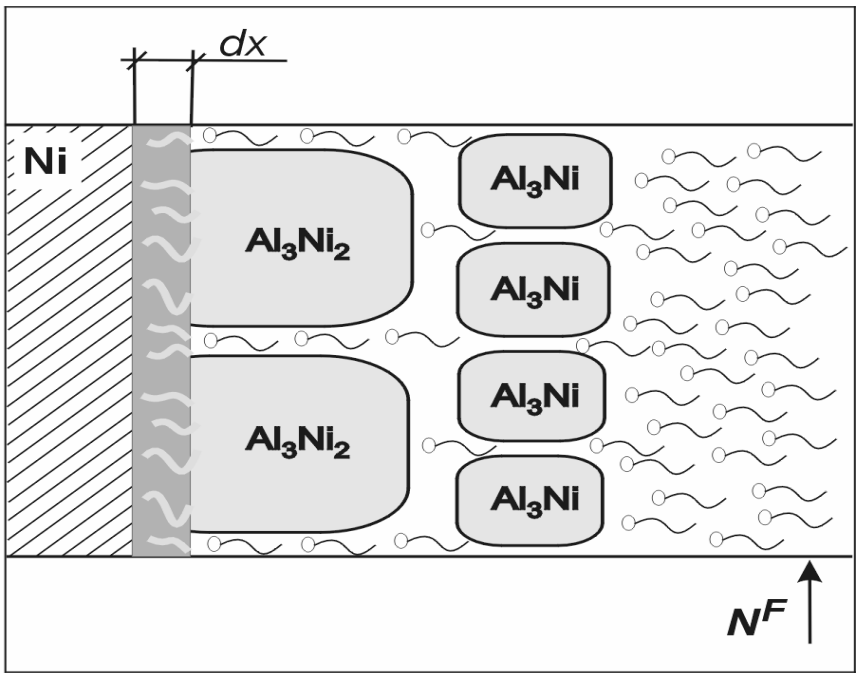

zone *dx* is formed
just at the surface of substrate

the liquid N^F reacted with substrate Ni
so long as zone, *dx,* becomes liquid
the reaction leads to creation of the
solute concentration equal to the N_0
the value of the N_0 depends on
the real temperature, T_R,
imposed by technology

cellular morphology of sub-layers

FIG. 18

liquid (N^F) + substrate (Ni) → undercooled liquid (N_0)

the liquid (N^F) diffuses along the channels between cells

Undercooled peritectic reactions Metastable conditions

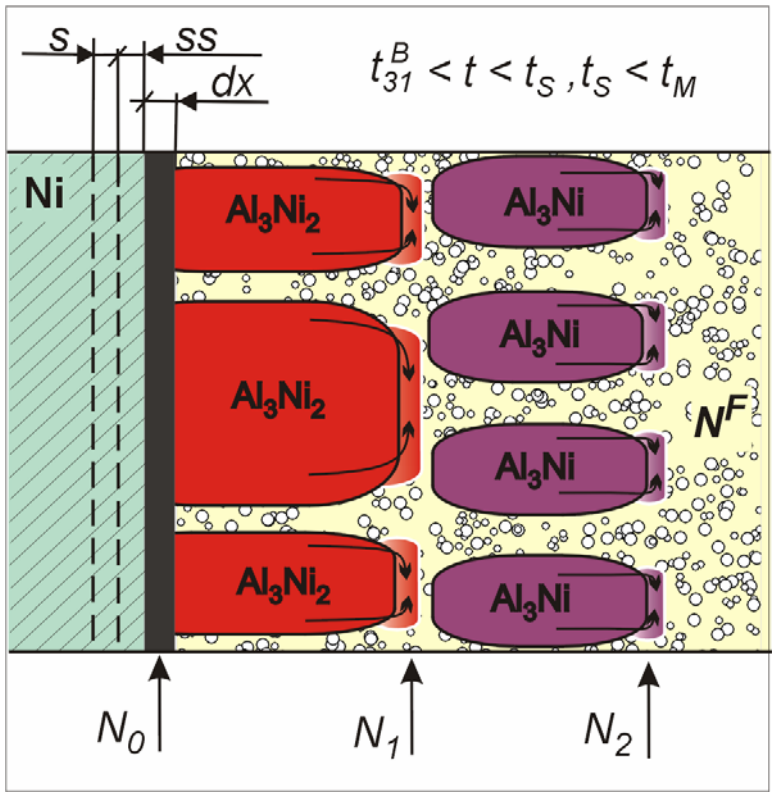

undercooled liquid (N_0) diffuses along internal channels towards the solid/liquid interface of cells dominant phase solidifies due to first undercooled peritectic reaction coupled phase solidifies due to second undercooled peritectic reaction

solidification is completed at time, t_S

at time, t_M, first solid / solid transformation takes place

FIG. 19 peritectic reactions

undercooled peritectic reaction under metastable conditions can also be described by reaction resulting from phase diagram for stable equilibrium: primary phase + liquid ➔ peritectic phase

Undercooled peritectic reactions Metastable conditions

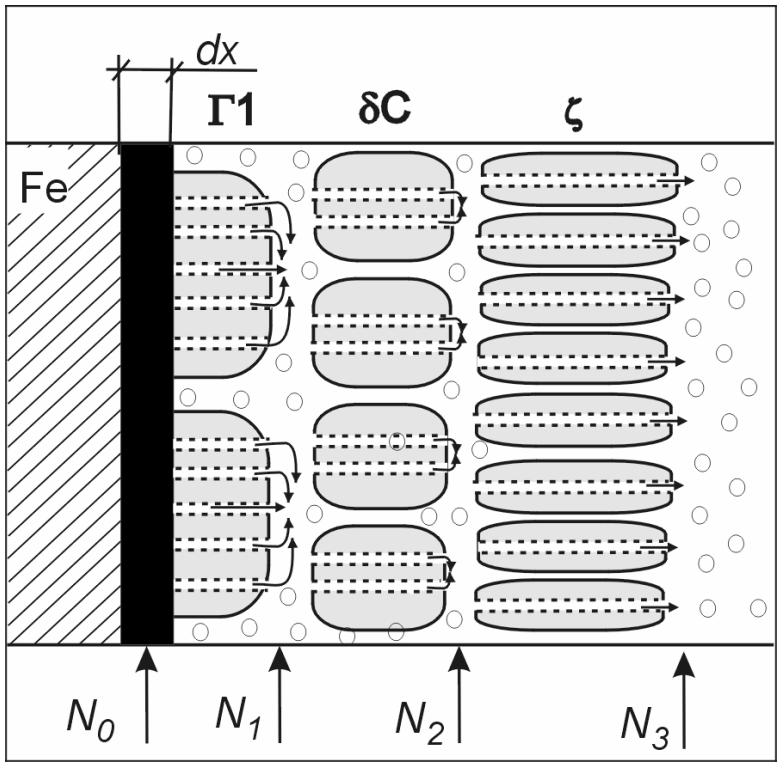

undercooled liquid (N_0) diffuses along internal channels towards the solid/liquid interface of cells

peritectic reactions
Fe/Zn/Fe joint

FIG. 20

undercooled peritectic reaction under metastable conditions can also be described by reaction resulting from phase diagram for stable equilibrium: **primary phase + liquid ➔ peritectic phase**

Completion of solidification

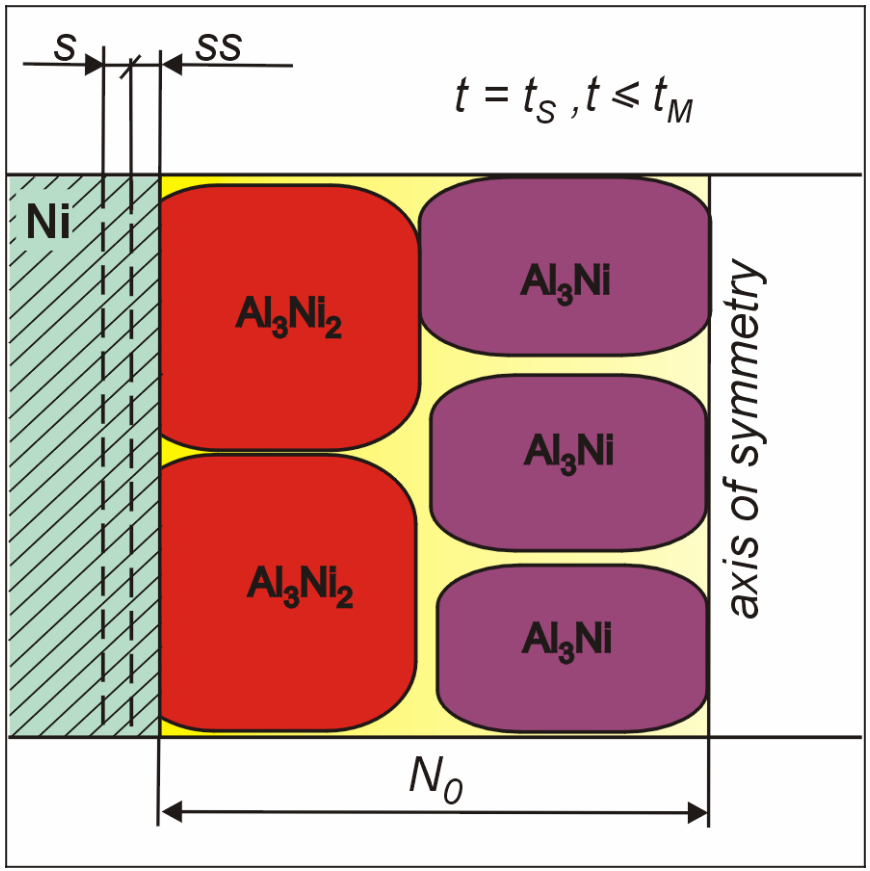

FIG. 21

each sub-layer consists of cells

- **no more zone *dx***
- **ss zone remains**
- **s zone remains**
- **both sub-layers are fully formed**
- **N_0 concentration is conserved due to mass balance**
- **channels still exist internal & external**
- **no more N^F - liquid**

CONCLUSION: time t_S depends on thickness of foil applied for joining

Operating range for solidification

FIG. 22

operating range

model referred to phase diagram for stable equilibrium

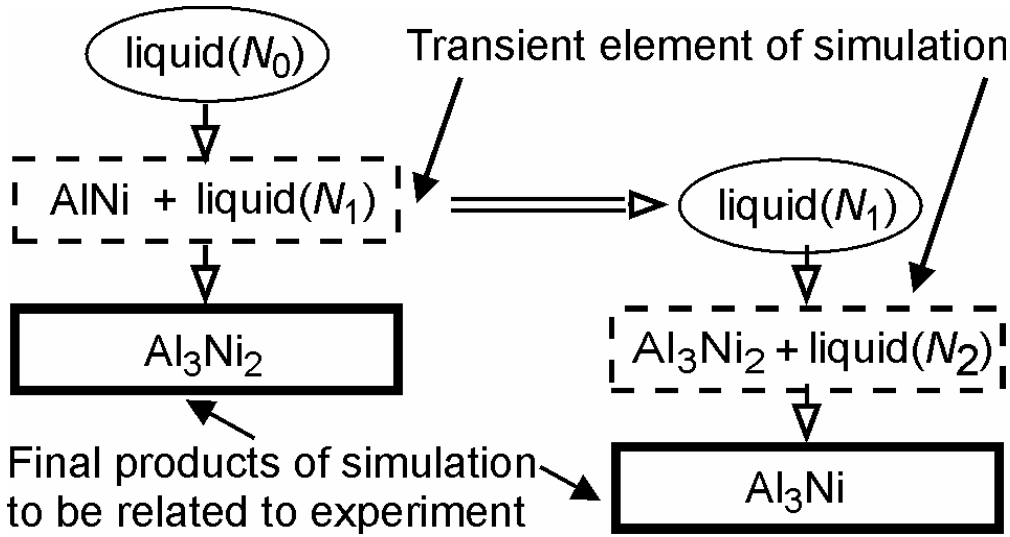

formation of Al_3Ni_2–Al_3Ni multi-layer on Ni - substrate
formation of multi-layer follows mechanism of
undercooled peritectic reactions at T_R technological temperature
according to phase diagram for stable equilibrium:
primary (AlNi) + *liquid* (N_1) → Al_3Ni_2
primary (Al_3Ni_2) + *liquid* (N_2) → Al_3Ni

Solidification path

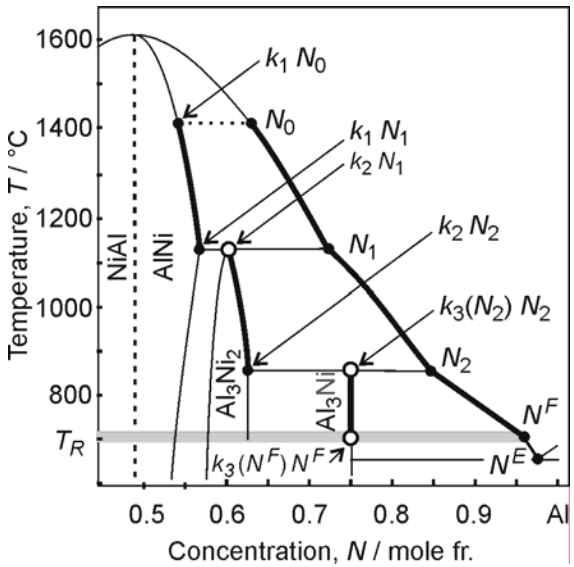

Ni-Al phase diagram

FIG. 23

FIG. 24

Fe-Zn phase diagram

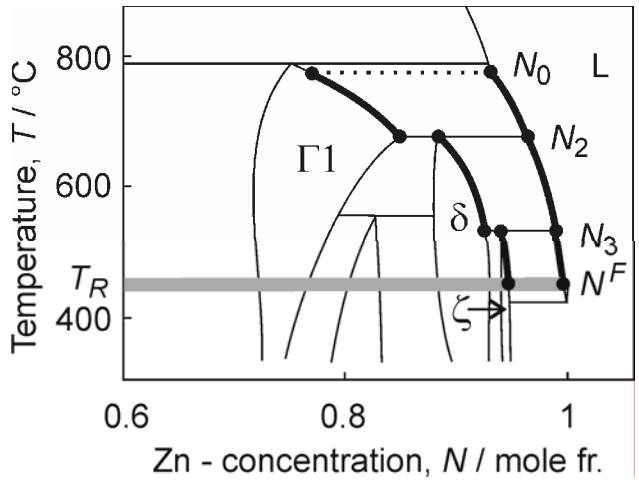

reduced $N_0 \rightarrow N_1 \rightarrow N_2$ and full $N_0 \rightarrow N_1 \rightarrow N_2 \rightarrow N^F$ solidification path;
reduced $k_1N_0 \rightarrow k_1N_1 \rightarrow k_2N_1 \rightarrow k_2N_2$
and full $k_1N_0 \rightarrow k_1N_1 \rightarrow k_2N_1 \rightarrow k_2N_2 \rightarrow k_3N_2 \rightarrow k_3N^F$
historical, N^S, s/l interface path Ni/Al/Ni

a peritectic reaction occurs at the end of a given solidification range

Redistribution coefficient, β

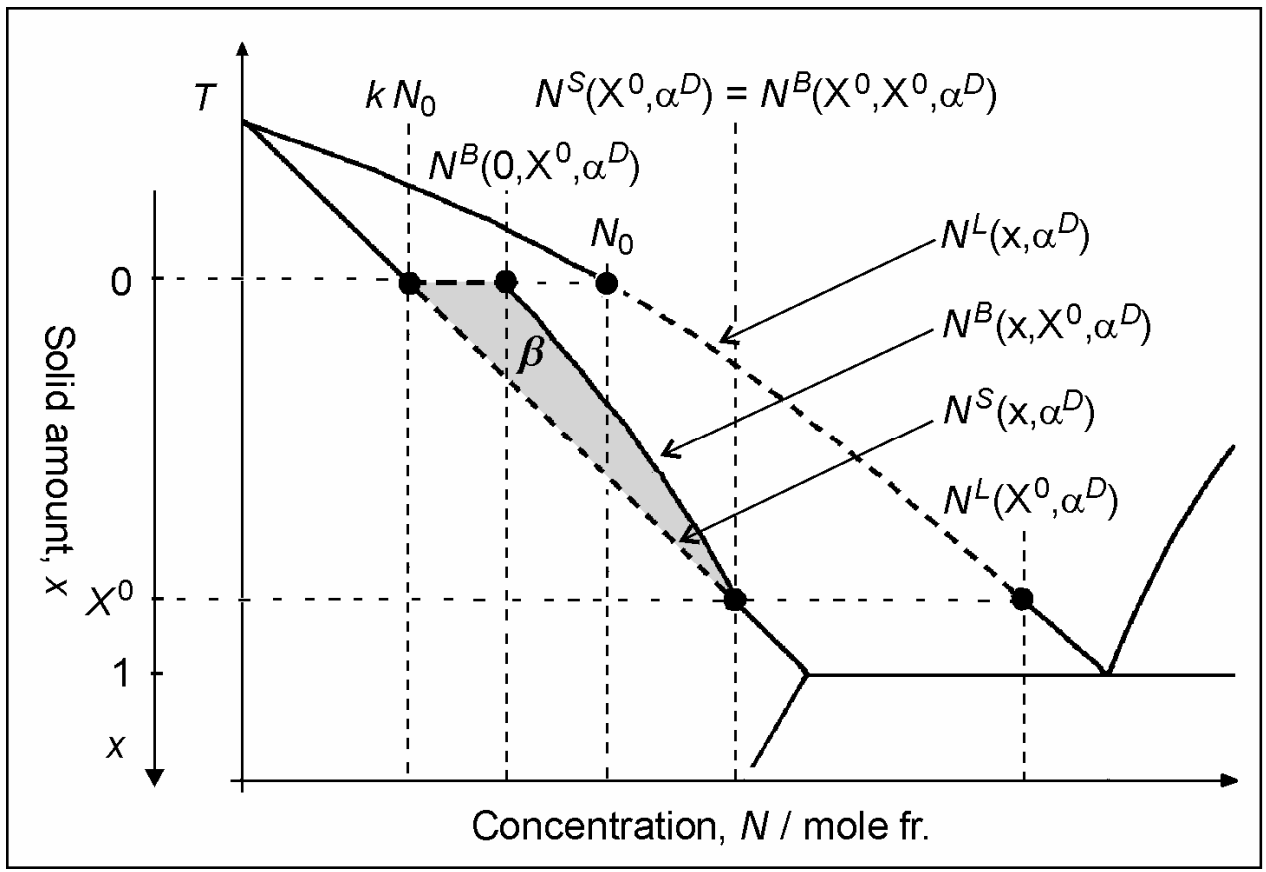

arbitrary phase diagram

N^L
solute concentration in the liquid
N^S
solute concentration at the s/l interface
N^B
solute redistribution after back diffusion

FIG. 25

Back-diffusion parameter, α

back-diffusion parameter
arbitrary phase diagram

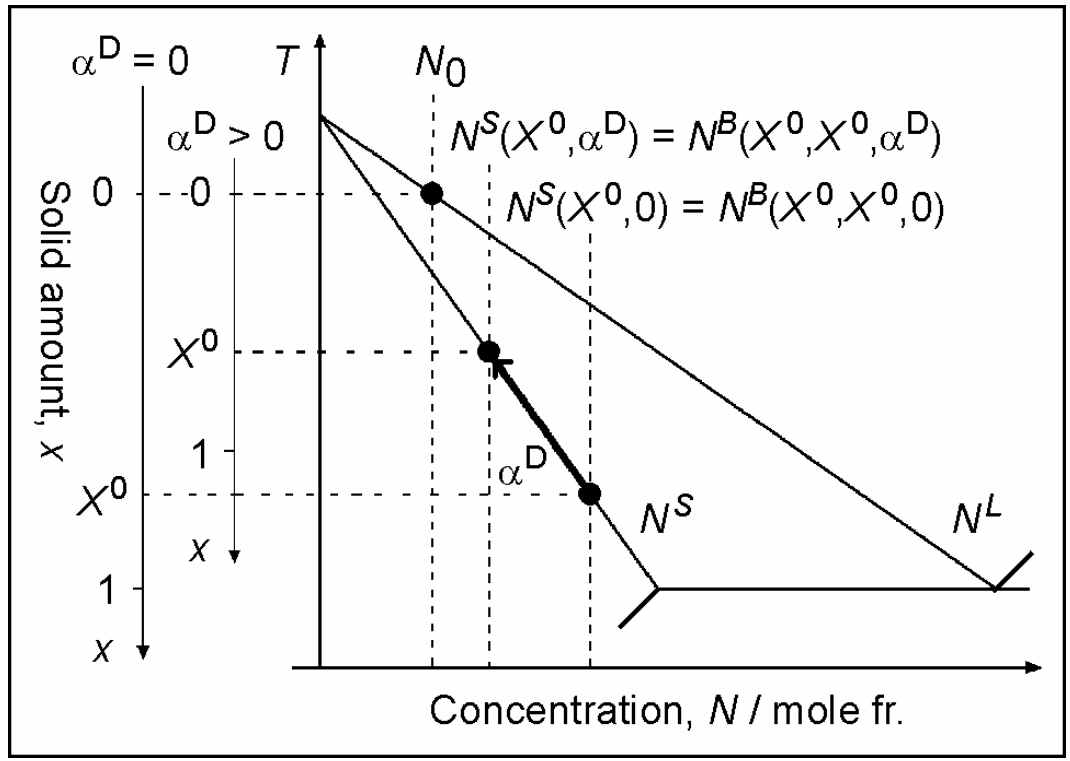

FIG. 26

$\alpha^D = 0$ axis corresponding to the Scheil's theory
$\alpha^D > 0$ axis corresponding to the general model for solidification / microsegregation

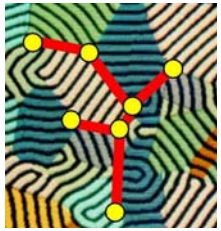

Equations

$$k_i(N_i^L) = k_i^0 + k_i^L \frac{N_{i-1}}{N_i^L}$$

universal definition of partition ratio

$$x_i + liquid(N_i) \Rightarrow \left[x_i^{\max} - x_i^{\min} \right]$$

amount of peritectic phase due to reaction resulting from phase diagram

$$x_i\,(\alpha_i^D, l_i^0, N_{i-1}, N_i, k_i) = l_i^0\,[1-\alpha_i^D\,k_i]^{-1}\,\left[1-\left(N_i/N_{i-1}\right)^{\frac{1-\alpha_i^D\,k_i}{k_i-1}}\right]$$

amount of primary phase

$$\frac{dN_i^L}{dx} = \frac{(1-k_i^0)\,N_i^L - k_i^L\,N_{i-1}}{l_i^0 + \alpha_i^D\,k_i^0\,x - x}$$

differential equation governing solidification / microsegregation

$$N_i^L(0, \alpha_i^D, l_i^0, N_{i-1}, k_i^0) = N_{i-1}$$

initial condition

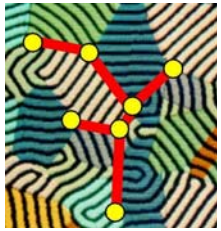

Equations

$$N_i^L\left(x,\alpha_i^D,l_i^0,N_{i-1},k_i\right)=\frac{N_{i-1}}{1-k_i^0}\left\{k_i^L+(1-k_i^0-k_i^L)\left[(l_i^0+\alpha_i^D\,k_i^0\,x-x)/l_i^0\right]^{\frac{k_i^0-1}{1-\alpha_i^D\,k_i^0}}\right\}$$

$$N_i^S(x,\alpha_i^D,l_i^0,N_{i-1},k_i)=k_i^0\;N_i^L\left(x,\alpha_i^D,l_i^0,N_{i-1},k_i\right)+k_i^L N_{i-1}$$

$$N_i^B\left(x,x_i^0,\alpha_i^D,l_i^0,N_{i-1},k_i^0\right)=\left[1+\beta_i^{ex}(x,x_i^0,l_i^0,k_i^0)\;\beta_i^{in}(x_i^0,\alpha_i^D,l_i^0,k_i^0)\right]N_i^S(x,\alpha_i^D,l_i^0,N_{i-1},k_i^0)$$

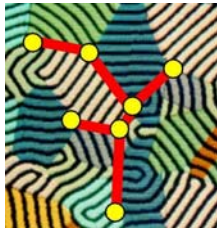

Equations

$$\beta_i^{ex}\left(x, x_i^0, l_i^0, k_i\right) = \frac{k_i^0\, l_i^0\, (1 - k_i^0 - k_i^L)\, (x_i^0 - x)}{(l_i^0 + k_i^0\, x_i^0 - x_i^0)(k_i^0\, l_i^0 + k_i^L\, l_i^0 - k_i^L\, x)}$$

$$\beta_i^{in}\left(x_i^0, \alpha_i^D, l_i^0, k_i\right) = \left[a_3\, k_i^L\, (1 - k_i^0)(a_4 - l_i^0\, N_{i-1} + x_i^0)(l_i^0 + k_i^0\, x_i^0 - x_i^0)(\alpha_i^D - 1)\right] \times$$
$$\left[a_2\, a_3\, l_i^0\, k_i^0\, N_{i-1}\left(a_2\, l_i^0 + k_i^L x_i^0 (\alpha_i^D - 1) + a_5\, (k_i^0 l_i^0 + k_i^L l_i^0 - k_i^L x_i^0)(\alpha_i^D - 1)\right) + \right.$$
$$\left. a_1\, a_2^2\, N_{i-1}(a_6\, f_2 - a_3\, l_i^0\, k_i^0)(l_i^0 + \alpha_i^D k_i^0 x_i^0 - x_i^0) - a_2^2\, a_6\, f_1\, l_i^0\, N_{i-1}\right]^{-1}$$

β^{ex} coefficient of the extent of redistribution

β^{in} coefficient of the intensity of redistribution

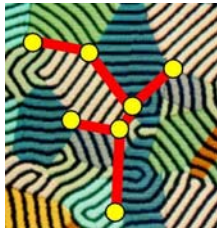

Equations

$$ {}_2F_1(a,b,c,x) = 1 + \frac{a\,b\,x}{1!c} + \frac{a(a+1)b(b+1)x^2}{2!c(c+1)} + \cdots = \sum_{k=0}^{\infty} \frac{(a)_k\,(b)_k\,x^k}{(c)_k\,k!} $$

$$ f_1 = {}_2F_1\left(\frac{\alpha_i^D k_i^0 - k_i^0}{\alpha_i^D k_i^0 - 1}, 1; \frac{2\alpha_i^D k_i^0 - k_i^0 - 1}{\alpha_i^D k_i^0 - 1}; \frac{k_i^L}{k_i^0(\alpha_i^D k_i^0 + \alpha_i^D k_i^L - 1)} \right) $$

$$ f_2 = {}_2F_1\left(\frac{\alpha_i^D k_i^0 - k_i^0}{\alpha_i^D k_i^0 - 1}, 1; \frac{2\alpha_i^D k_i^0 - k_i^0 - 1}{\alpha_i^D k_i^0 - 1}; \frac{k_i^L (l_i^0 + \alpha_i^D k_i^0 x_i^0 - x_i^0)}{k_i^0 l_i^0 (\alpha_i^D k_i^0 + \alpha_i^D k_i^L - 1)} \right) $$

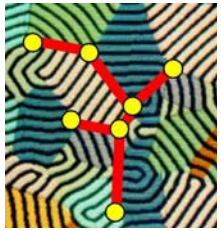

Equations

$$a_1 = \left[\left(l_i^0 + \alpha_i^D k_i^0 x_i^0 - x_i^0 \right) / l_i^0 \right]^{\frac{k_i^0 - 1}{1 - \alpha_i^D k_i^0}}$$

$$a_2 = k_i^0 + k_i^L - 1$$

$$a_3 = k_i^0 \alpha_i^D + k_i^L \alpha_i^D - 1$$

$$a_4 = \frac{N_{i-1} \left(l_i^0 - x_i^0 \right) \left(k_i^L - a_1 a_2 \right)}{1 - k_i^0}$$

$$a_5 = \ln \frac{k_i^0 l_i^0 + k_i^L l_i^0 - k_i^L x_i^0}{k_i^0 l_i^0 + k_i^L l_i^0}$$

$$a_6 = \left(k_i^0 l_i^0 + k_i^L l_i^0 - k_i^L x_i^0 \right) \left(\alpha_i^D k_i^0 - 1 \right)$$

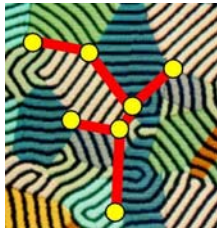

Equations

for $k_i^L = 0$

$$x_i^{max}(x_i^0, \alpha_i^D, \alpha_i^P, l_i^0, N_{i-1}, N_i, k_i^0, k_{i+1}^0) = x_i^{mem}(x_i^0, \alpha_i^D, \alpha_i^P, l_i^0, N_{i-1}, N_i, k_i^0, k_{i+1}^0);$$

$$when \quad r_i(\alpha_i^D, l_i^0, N_{i-1}, N_i, k_i^0, k_{i+1}^0) > (N_i - k_{i+1}^0 N_i) \times$$

$$\left[x_i^{mem}(x_i^0, \alpha_i^D, \alpha_i^P, l_i^0, N_{i-1}, N_i, k_i^0, k_{i+1}^0) - x_i(\alpha_i^D, l_i^0, N_{i-1}, N_i, k_i^0)\right]$$

with

$$r_i(\alpha_i^D, l_i^0, N_{i-1}, N_i, k_i^0, k_{i+1}^0) = k_{i+1}^0 N_i \, x_i(\alpha_i^D, l_i^0, N_{i-1}, N_i, k_i^0) - \int_0^{x_i} N_i^B(x, x_i, \alpha_i^D, l_i^0, N_{i-1}, k_i^0)\, dx$$

and

Equations

$$x_i^{mem}(x_i^0,\alpha_i^D,\alpha_i^P,l_i^0,N_{i-1},N_i,k_i^0,k_{i+1}^0)=\min\Big\{x_i^0;\ x_i(\alpha_i^D,l_i^0,N_{i-1},N_i,k_i^0)+$$
$$\left[x_i(\alpha_i^P,l_i^0,k_{i+1}^0N_i,N_i,k_{i+1}^0)-x_i(\alpha_i^P,l_i^0,k_{i+1}^0N_i,N_i,k_i^0)\right]\times$$
$$\left[x_i(\alpha_i^P,l_i^0,k_{i+1}^0N_i,N_i,k_i^0)-x_i(0,l_i^0,k_{i+1}^0N_i,N_i,k_i^0)\right]\times$$
$$\left[x_i(1,l_i^0,k_{i+1}^0N_i,N_i,k_i^0)-x_i(0,l_i^0,k_{i+1}^0N_i,N_i,k_i^0)\right]^{-1}\Big\}$$

it yields

$$x_i^{max}(x_i^0,\alpha_i^D,\alpha_i^P,l_i^0,N_{i-1},N_i,k_i^0,k_{i+1}^0)=x_i(\alpha_i^D,l_i^0,N_{i-1},N_i,k_i^0)+$$
$$r_i(\alpha_i^D,l_i^0,N_{i-1},N_i,k_i^0,k_{i+1}^0)\Big/(N_i-k_{i+1}^0N_i);$$
$$when\quad r_i(\alpha_i^D,l_i^0,N_{i-1},N_i,k_i^0,k_{i+1}^0)\le(N_i-k_{i+1}^0N_i)\times$$
$$\left[x_i^{mem}(x_i^0,\alpha_i^D,\alpha_i^P,l_i^0,N_{i-1},N_i,k_i^0,k_{i+1}^0)-x_i(\alpha_i^D,l_i^0,N_{i-1},N_i,k_i^0)\right]$$

Equations

and

$$\int_0^{x_i^{min}} \left[N_i^B(x + x_i - x_i^{min}, x_i, \alpha_i^D, l_i^0, N_{i-1}, k_i^0) - N_i^B(x, x_i, \alpha_i^D, l_i^0, N_{i-1}, k_i^0) \right] dx +$$

$$\int_{x_i^{min}}^{x_i} \left[k_{i+1}^0 N_i - N_i^B(x, x_i, \alpha_i^D, l_i^0, N_{i-1}, k_i^0) \right] dx =$$

$$(N_i - k_{i+1}^0 N_i) \left[x_i^{max}(x_i^0, \alpha_i^D, \alpha_i^P, l_i^0, N_{i-1}, N_i, k_i^0, k_{i+1}^0) - x_i(\alpha_i^D, l_i^0, N_{i-1}, N_i, k_i^0) \right]$$

however

$$\lambda_1^K / \lambda_2^K = \lambda_{32}^K / \lambda_{31}^K \cong \left(x_1^{\max} - x_1^{\min} \right) / \left(x_2^{\max} - x_2^{\min} + x_3 \right)$$

above equation is connected with the scheme shown in FIG. 8a

Simulation

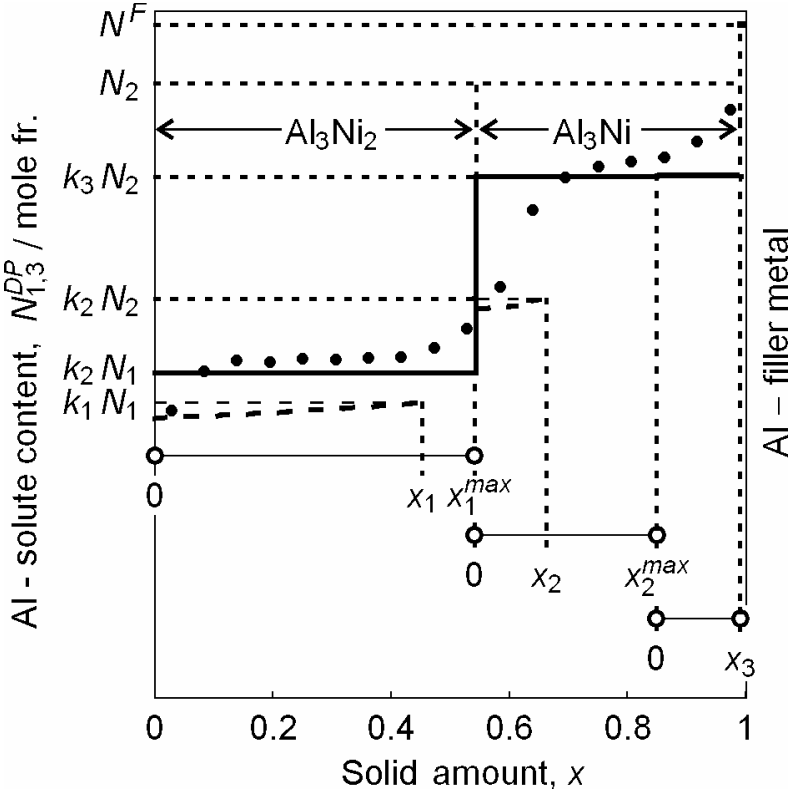

FIG. 27

reproduction of planar (constant) profile of solute concentration (redistribution) and ratio of sub-layers thickness according to the operating range FIG. 22 and full solidification path (phase diagram for stable equilibrium)

points come from EDS measurement solidification arrested after 121 s

$$\lambda_1^K / \lambda_2^K = \lambda_{32}^K / \lambda_{31}^K \cong \left(x_1^{\max} - x_1^{\min}\right) / \left(x_2^{\max} - x_2^{\min} + x_3\right)$$

First solid / solid transformation

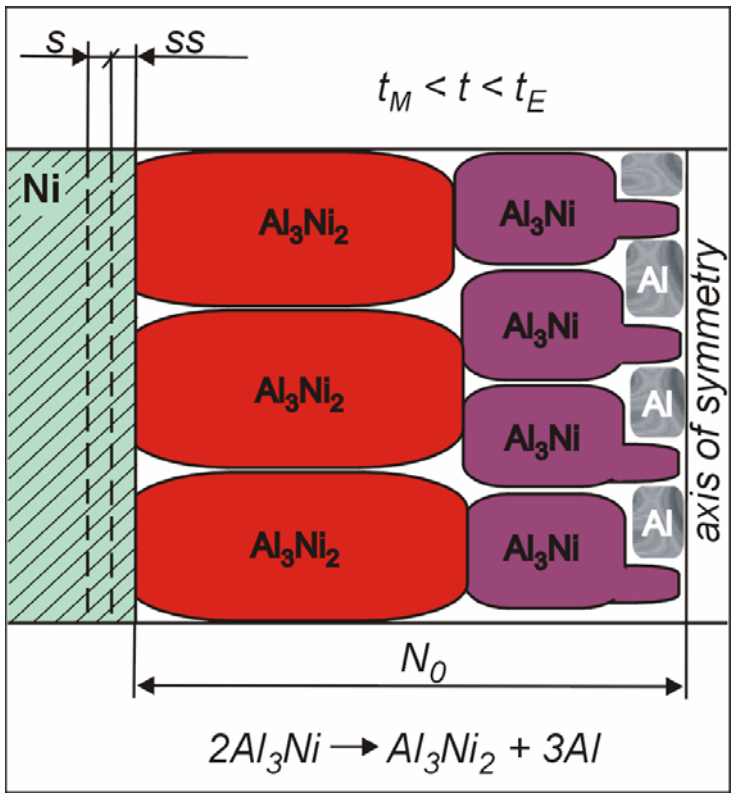

FIG. 28

first solid/solid transformation:

$2\,Al_3Ni \rightarrow Al_3Ni_2$ + liquid (3Al)

liquid (Al) precipitates and diffuses towards the axis of symmetry of joint

N_0 is conserved during first solid/solid transformation

when transformation is arrested
then liquid (Al) shrinks and pores appear

first solid / solid transformation named as a *„mantis"* effect

RESULT time t_M
seems to be typical for a given system

First solid / solid transformation Experimental confirmation

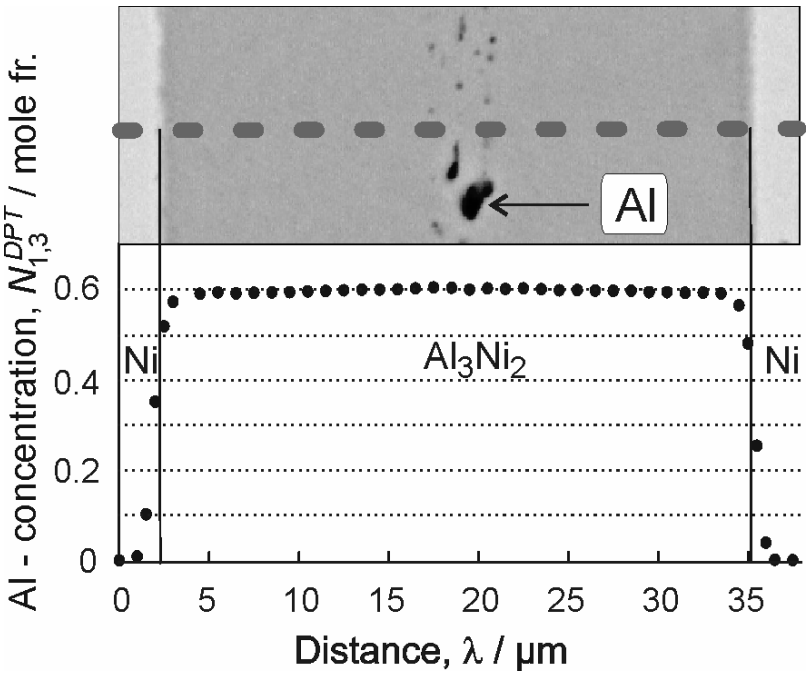

FIG. 29 first solid / solid transformation within Ni/Al/Ni joint

← by courtesy of Dr J. Janczak-Rusch, EMPA, Dübendorf, Switzerland

liquid (Al) precipitated at the axis of symmetry of joint

as observed

number of degrees of freedom
f = 0
according to Gibbs Phase Rule

$$f = c - p + 1 = 0$$

since
c = 2 Ni, Al
p = 3 precipitated liquid (Al), Al_3Ni_2, Al_3Ni

First solid / solid transformation Experimental confirmation

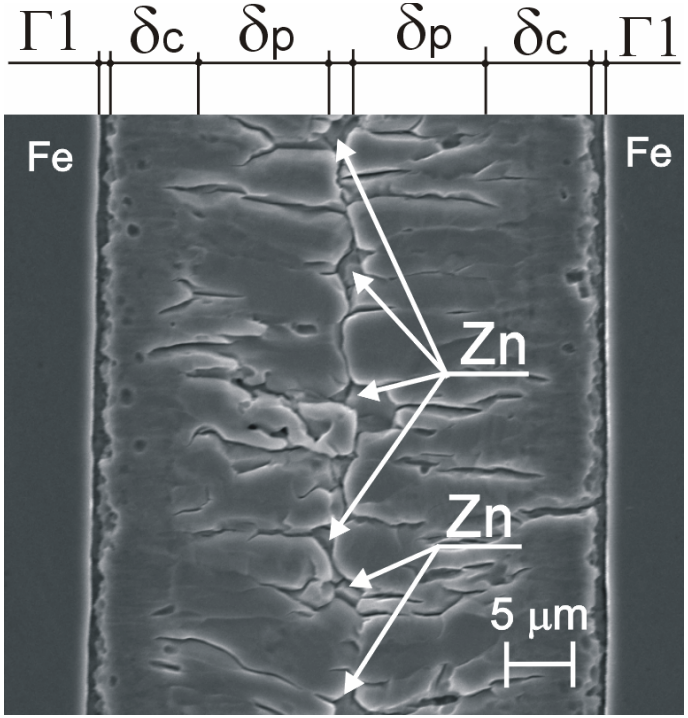

FIG. 30

first solid / solid transformation within Fe/Zn/Fe joint

←by courtesy of Prof. E.Guzik and Dr D. Kopyciński, University of Science and Technology, Kraków, Poland

$FeZn_{13}$ ➔ $FeZn_{10}$ + *liquid* (3Zn)

ζ ➔ δ + *liquid (3Zn)*

liquid (Zn) precipitated at the axis of symmetry of joint

as observed

number of degrees of freedom

$f = c - p + 1 = 0$

since

c = 2 Fe, Zn

p = 3 precipitated (Zn), δ, ζ

Simulation

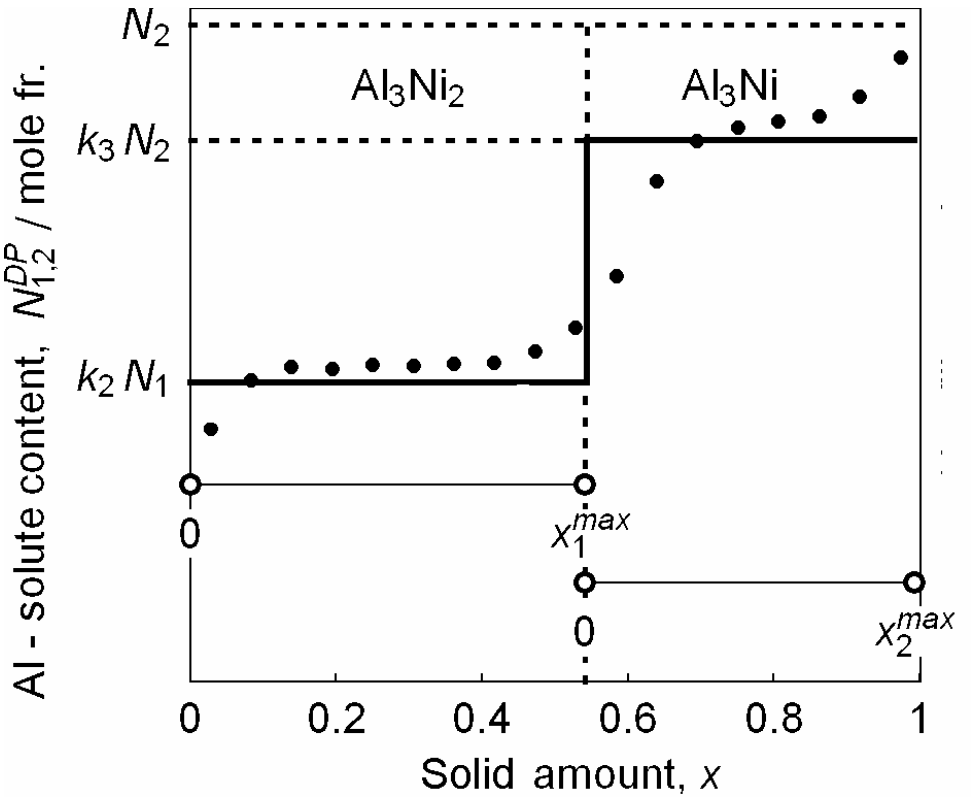

FIG. 31

reproduction of the Al-solute redistribution across Al_3Ni_2–Al_3Ni multi-layer being in the contact with a Ni – substrate
reduced solidification path; model referred to phase diagram for stable equilibrium

RESULT plane profile of simulated redistribution, $k_{i+1}N_i$, is obtainable, only

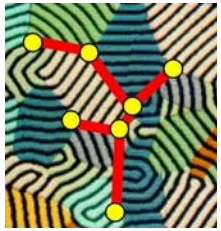

Simulation

FIG. 32

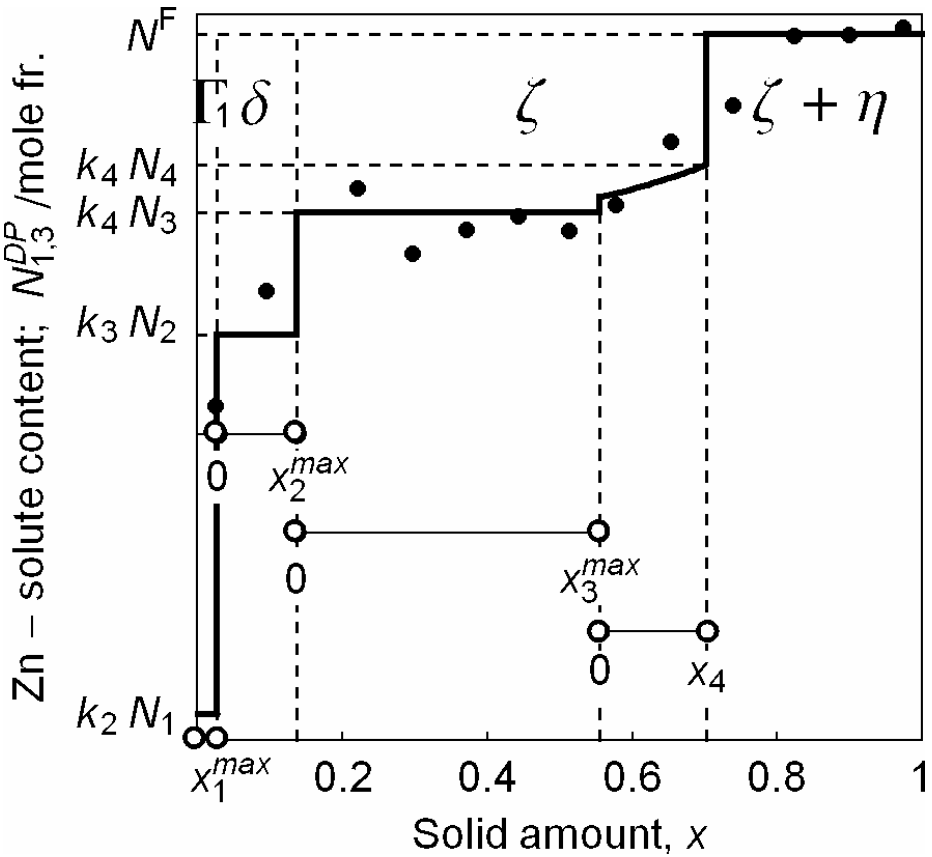

reproduction of the Zn-solute redistribution across δ–ζ multi-layer being in the contact with a (Γ_1 + Fe) – substrate
full solidification path;
model referred
to phase diagram
for stable equilibrium

RESULT plane profile of simulated redistribution, $k_{i+1}N_i$, is obtainable, only

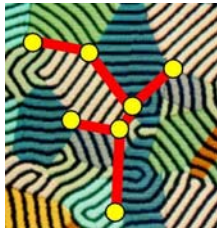

Sequence

sequence of phase appearance during solidification according to

1/ the *dx* model (simulation):
first Al_3Ni_2 next Al_3Ni

2/ phase diagram for stable equilibrium (peritectic reactions):
first Al_3Ni_2 next Al_3Ni

3/ the birth: FIG. 16
first Al_3Ni_2 next Al_3Ni

4/ criterion of maximum temperature of the s / l interface (metastable conditions):
first Al_3Ni_2 next Al_3Ni

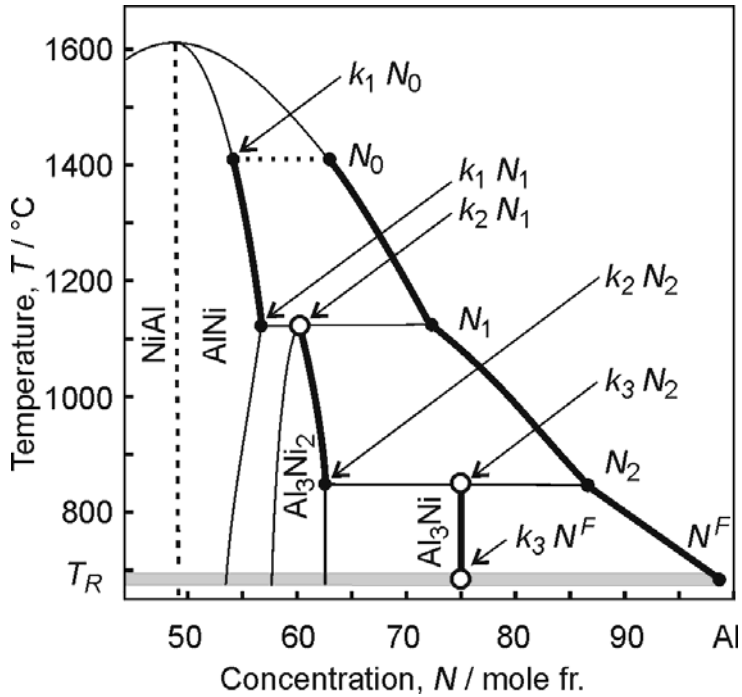

FIG. 33

full solidification path; phase diagram for stable equilibrium formation of peritectic phases:
primary x_i + liquid (N_i) ➔ $k_{i+1}N_i$

Sequence
Theorem of maximum driving force

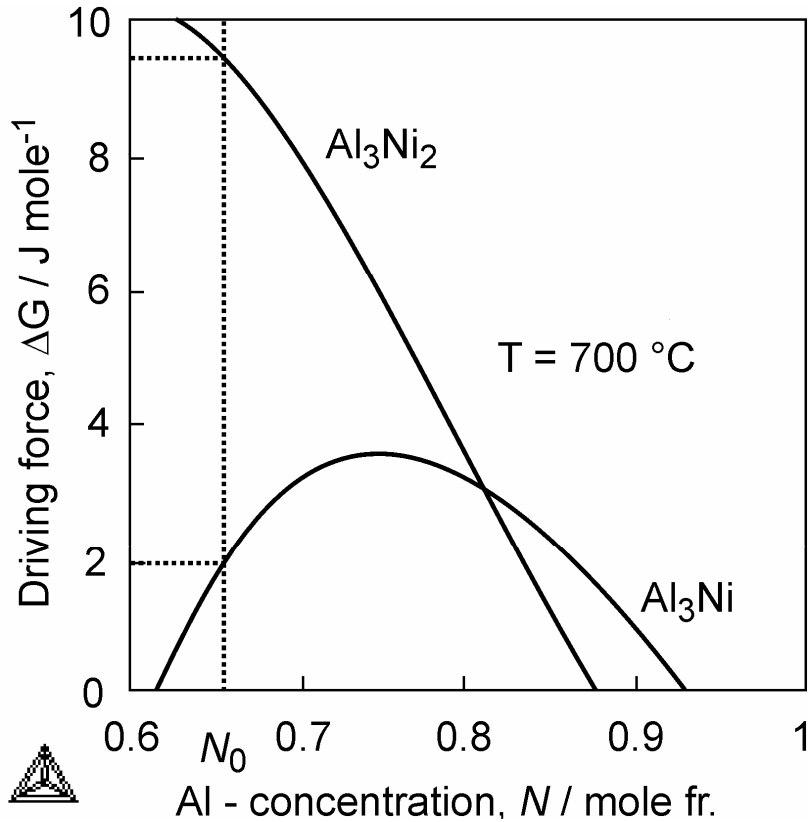

FIG. 34

the dominant phase Al_3Ni_2 appears first during solidification

by courtesy of Dr J. Golczewski, Senior Scientist
Max-Planck Institut für Metallforschung, Stuttgart, Germany

Sequence
Theorem of maximum driving force

the coupled phase Al_3Ni
is consumed by
the dominant phase Al_3Ni_2
during first s/s transformation,
FIG. 35a

the dominant phase δ
appears first
during solidification
FIG. 35b

FIG. 35

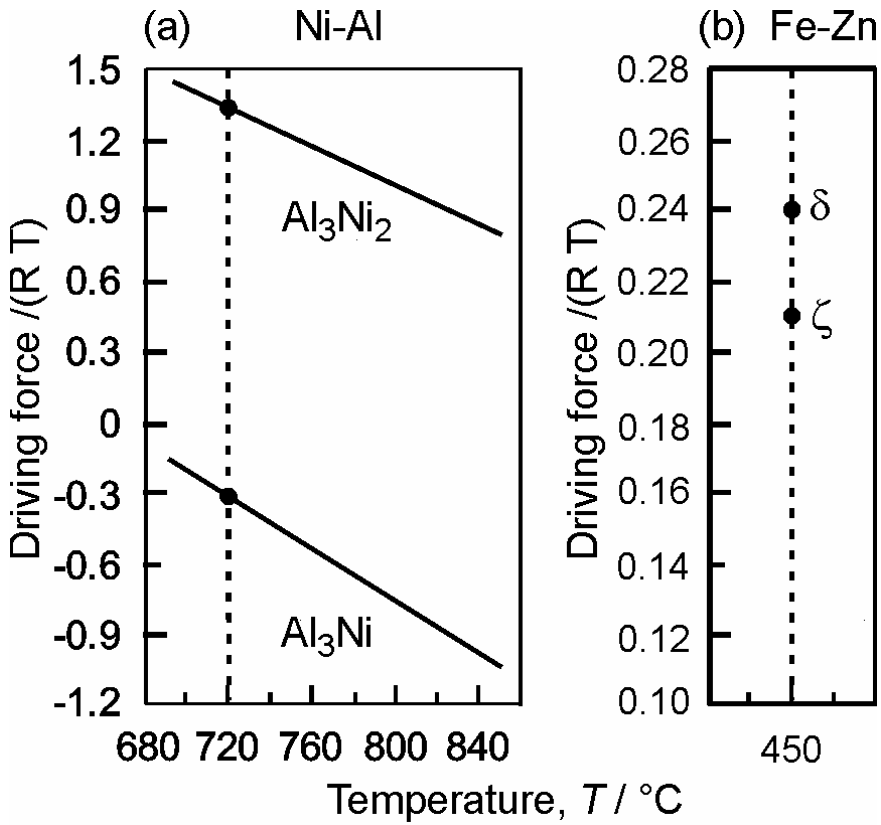

a/ first s/s transformation
b/ solidification

by courtesy of Prof. Hyuck-Mo Lee
Advanced Institute of Science and Technology, Yusung-Gu, Taejon, Korea

Arrested solidification
Frozen morphology

solidification arrested during the formation of the Ni-Al-Ni – joint

the thickening of the Al_3Ni intermetallic compound continues (due to an applied arresting) along solidification path:
$N^F \rightarrow N^E$, (FIG. 23)
this is accompanied by the appearance of an inter-layer of frozen $(Al)^M$
in the middle an eutectic: $[Al_3Ni+(Al)^S]$ is visible
the $(Al)^M$ and $(Al)^S$ phases are the metastable and stable eutectic phases, respectively

FIG. 36

thickening rate depends on crystallographic orientation of a given cell

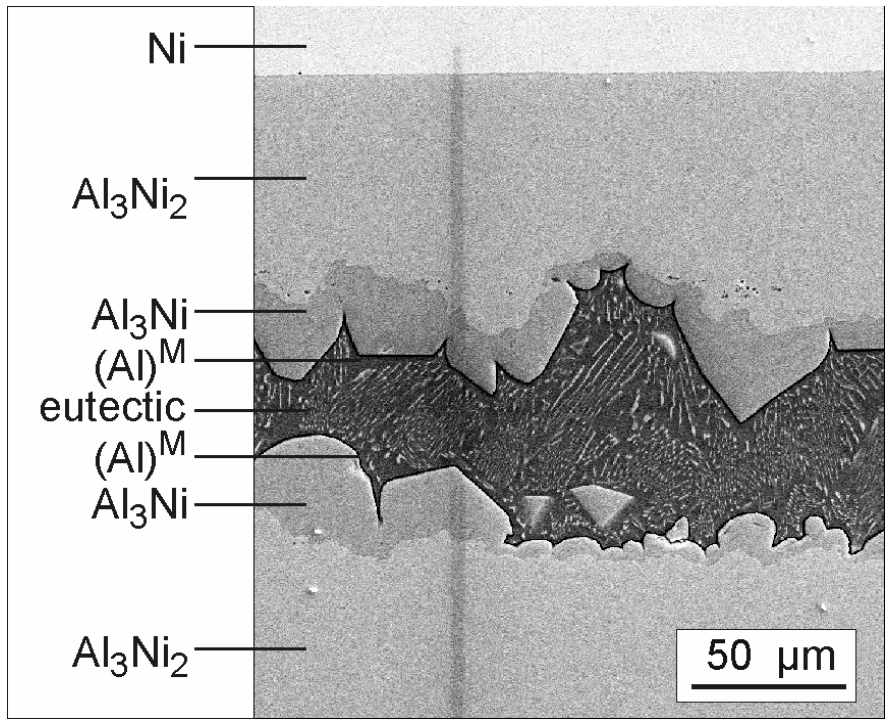

by courtesy of Dr J. Janczak-Rusch, EMPA, Dübendorf, Switzerland ➔

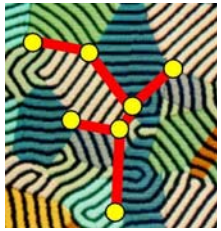

Concluding remarks

the current model equations could be successfully applied
to simulation with the use of phase diagram for metastable equilibrium
simulated profiles would be more flexible to fit perfectly
experimental points
each slope of measured profile would be reproducible

the present description is able to give information about
a value of diffusion coefficient, D_s
but analysis of the definition of back-diffusion parameter is needed

the proposed model could be developed for multi-component systems
but determination of solidification path becomes more complicated
as shown by H-W mode of calculation

H-W ➔ T. Himemiya, W. Wołczyński,
Materials Transactions, The Japan Institute of Metals, 43, (2002), 2890-2896

METRO
MEtallurgical TRaining On-line

Solidification / microsegregation model applied to description of diffusion soldering / brazing

End of the lecture

Education and Culture